

On the Distribution of AgBr Grains in Photographic Plates for Ion Detection in Mass-Spectrometers

H. W. WERNER and J. M. NIEUWENHUIZEN

Philips Research Laboratories, N. V. Philips' Gloeilampenfabrieken, Eindhoven, Netherlands

(Z. Naturforsch. **22 a**, 1035—1039 [1967]; received 1 March 1967)

Investigations have been carried out on the distribution of AgBr-grains in unexposed photographic plates (type Q2, Ilford Ltd.) used for ion detection in mass-spectrometers. Electron micrographs show that a large fraction of the grains protrude about halfway out of the gelatine matrix and that these grains are covered by a very thin gelatine layer on the side facing the ions. The mean projection area of the unexposed grains, the percentage of the plate area covered with unexposed grains, and the emulsion thickness have been determined. The shape of unexposed as well as exposed and developed grains is discussed. A model of the distribution of the AgBr-grains in the emulsion is presented.

Photographic plates are widely used for the detection of ions in mass-spectrometers and a number of studies have been carried out to arrive at a better understanding of the nature of ion detection¹ with these plates. So far, theories on this subject²⁻⁴ have been based on assumptions concerning the distribution of the silver-halide grains in the gelatine matrix. The purpose of the present investigation was to determine, mainly by means of an electron microscope, how the unexposed grains are distributed in the gelatine matrix in order to check in this way whether the assumptions made in the theories mentioned above were justified⁵.

Experimental Procedure

Direct Pt—C replicas from unexposed photographic plates were obtained in the usual way⁷. In order to obtain indirect Pt—C replicas for unexposed and also from developed photographic plates we used a thermoplastic⁸ (Technovit, Kulzer & Co.).

Electron micrographs of unexposed photographic plates are shown in Fig. 1 * (direct replica) and in Figs. 1 a and 1 b (indirect replicas, stereo-micrographs).

¹ For a survey see E. B. OWENS in A. J. AHEARN (ed.), *Mass Spectrometric Analysis of Solids*, Elsevier Publishing Co., Amsterdam—London 1966, p. 56.

² E. BURLEFINGER and H. EWALD, *Z. Naturforsch.* **16 a**, 430 [1961].

³ J. FRANZEN, K.-H. MAURER, and K. D. SCHUY, *Z. Naturforsch.* **21 a**, 37 [1966].

⁴ H. W. WERNER, *Philips Res. Repts.* **21**, 63 [1966].

⁵ FRANZEN and SCHUY have derived a theoretical formula³ describing the transparency curve of ion-sensitive photographic plates, based on a silver halide grain distribution in a gelatine matrix qualitatively similar to that found by the present authors. FRANZEN and SCHUY have measured hundreds of transparency curves⁶ and found that the agreement between their experimental curves and the theoretical curves

For replication of "nude" grains — i. e. grains bare of any gelatine skin — the gelatine of the photographic plate was dissolved in water at 50 degrees centigrade. After several cycles of washing and centrifugation the nude AgBr-grains were dispersed in water. Some drops of this dispersion were dried on a glass plate and a direct Pt—C replica made. Then the AgBr-grains were dissolved in $\text{Na}_2\text{S}_2\text{O}_3$. All critical manipulations were carried out in complete darkness.

Electron micrographs of the replicas were made with a Philips electron microscope, type EM 100 B, using stereo techniques for some of the exposures.

Unless otherwise stated, the properties of unexposed grains embedded in the gelatine of desiccated Q2-plates (Ilford Ltd.) emulsion number S 4339 will be discussed.

Studies by KLEIN⁹ on photographic plates have shown that the silver halide grains after exposure, form silver agglomerates during development, the shape and size of which depend on the method of development. FRANZEN et al.³ have shown for Q2-plates that, for developing times greater than 30 seconds, the average grain size is independent of the developer used and of its temperature. The sensitivity of these photographic plates being proportional to the mean projection area of unexposed grains, it seemed essential to us to study both unexposed and developed grains in order to find a relation between the size of the unexposed and the developed grains.

was, in the average, better than 0.6% relative standard deviation, indicating that the assumptions made by these authors are indeed correct.

⁶ K. D. SCHUY, private communication 1967.

⁷ See e. g. L. REIMER, *Elektronenmikroskopische Untersuchungsmethoden und Präparationsmethoden*, Springer-Verlag, Berlin 1959.

⁸ The procedure was as follows: a drop of fluid technovit was allowed to polymerize on the surface of the specimen thus forming a cast of the surface. This cast is detached from the surface and subsequently coated with Pt and C by vacuum-deposition. After dissolving the technovit the replica is ready for use in the electron microscope.

* Figs. 1, 3, 5, 6, 8 see pages 1036 a—d.

⁹ E. KLEIN, *Z. Elektrochem.* **62**, 505 [1958].



Unexposed Grains in the Photographic Plate

We call a grain "visible to ions" if, in an electron micrograph, it protrudes so far out of the gelatine matrix that its boundaries with its surroundings are distinctly recognizable and edges between crystal planes are cleanout¹⁰ (see additional sketch to Fig. 1).

As can be seen from Fig. 1, and even better from Figs. 1a + 1b by using a stereo viewer, a large percentage of the grains protrudes about halfway out of the gelatine matrix. The contours are found to be mainly hexagonal or triangular. On many of the grains the edges between adjacent crystal faces are so sharp that we may conclude that they can only be covered by a rather thin gelatine layer.

Fig. 2 shows a size-frequency distribution of the grains from an electron micrograph of an unexposed photographic plate. The projection areas of the individual unexposed grains were separately determined by means of a planimeter. We call N_0 the total number of grains within a given area A . The total area covered by these N_0 grains has been found in the first place by summing up all the individual projection areas of the N_0 grains. The value obtained in this way was checked by measuring the opacity $O = (\text{intensity of incident light})/(\text{intensity of transmitted light})$ of a transparent paper on which the area covered by the grains had been completely blackened with china ink.

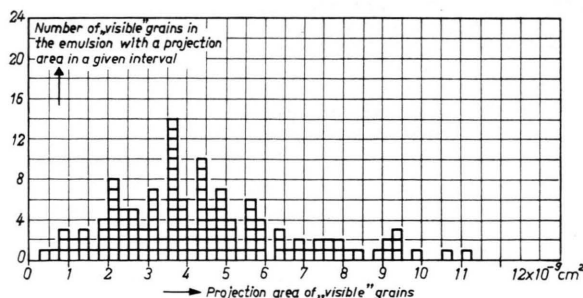


Fig. 2. Size-frequency distribution of "visible" grains in the emulsion.

¹⁰ We have assumed that an interaction between an impinging ion and a "grain visible to ions" takes place mainly by direct collisions between impinging ion and the atoms of the grain. As has been pointed out by FRANZEN and SCHUY, interaction between the impinging ion and the atoms of the grain may moreover take place via secondary processes, e. g. collision chains, etc. (see footnotes 17 and 36 of reference ³).

The mean projection area a_0 of unexposed grains has been determined as $a_0 = (\text{total area covered by } N_0 \text{ grains})/(\text{total number } N_0 \text{ of grains})$. We have thus found $a_0 = 4.0 \times 10^{-9} \text{ cm}^2$, which can also be estimated from Fig. 2.

Furthermore, by means of opacity measurements as described above we have determined the mean projection area of the grains from other regions on the same plate, and also from other plates (with the same emulsion number).

The deviations from the value given above lie within the experimental precision of the method and seem to be due mainly to the subjective decision whether a grain is assumed to be visible or not.

The fraction of the area covered by N_0 grains within a given area A is $(N_0 a_0)/A = a_0 G_0$. This quantity has been determined from many regions on the same plate as well as on different plates and was found to be 0.70 ± 0.07 ¹¹.

As can be seen from Fig. 1, the cross-section of the unexposed grains may in zeroth-order approximation be described as circles, the average diameter $D_0 = \{(4/\pi) a_0\}^{1/2}$ of which has been determined as $D_0 = 0.7 \mu\text{m}$.

Nude Grains

The nude grains were obtained by the procedure described above. An electron micrograph of these grains is shown in Fig. 3 and a size distribution in Fig. 4. The mean projection area a_n of the nude grains, as well as their diameter D_n , have been determined in the same way as a_0 and D_0 . We have found $a_n = 3.3 \times 10^{-9} \text{ cm}^2$, $D_n = 0.65 \mu\text{m}$.

The height h of the nude grains can be calculated from the shadows obtained by evaporating Pt at an angle of 30° (measured against the plane of the support) on to the grains and its support. The average height h determined from Fig. 3 was $h = 0.7 \mu\text{m}$, which is almost the same as the diameter D_n , i. e. the nude grains may in zero-order approximation be considered as being spherical. As the shape of the grains is not changed during the procedure which

¹¹ From this it can be concluded that at least for the batch of plates we have used, the sensitivity of the photographic plates should not vary more than $\pm 10\%$ on one plate or on different plates if it were only dependent on the distribution of visible grains.

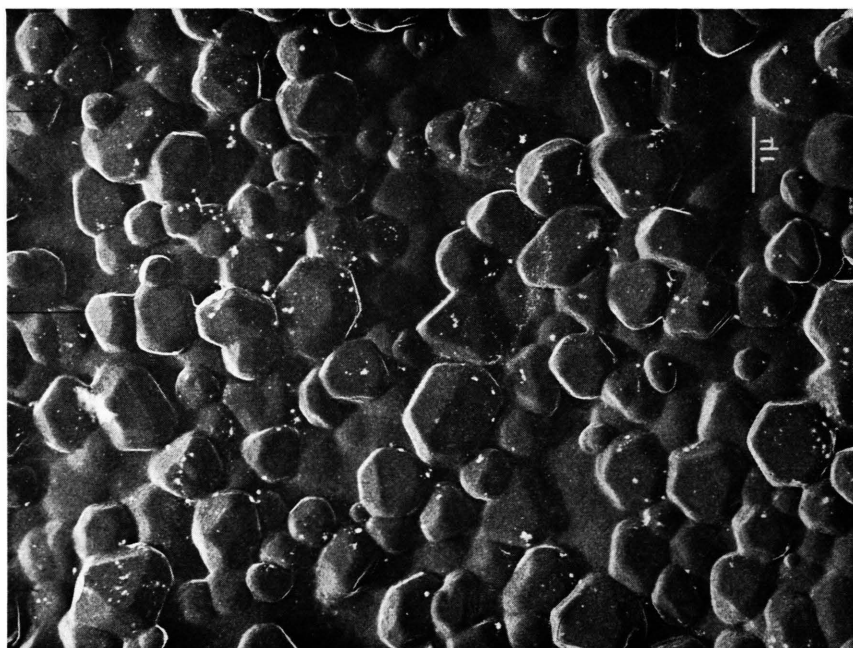
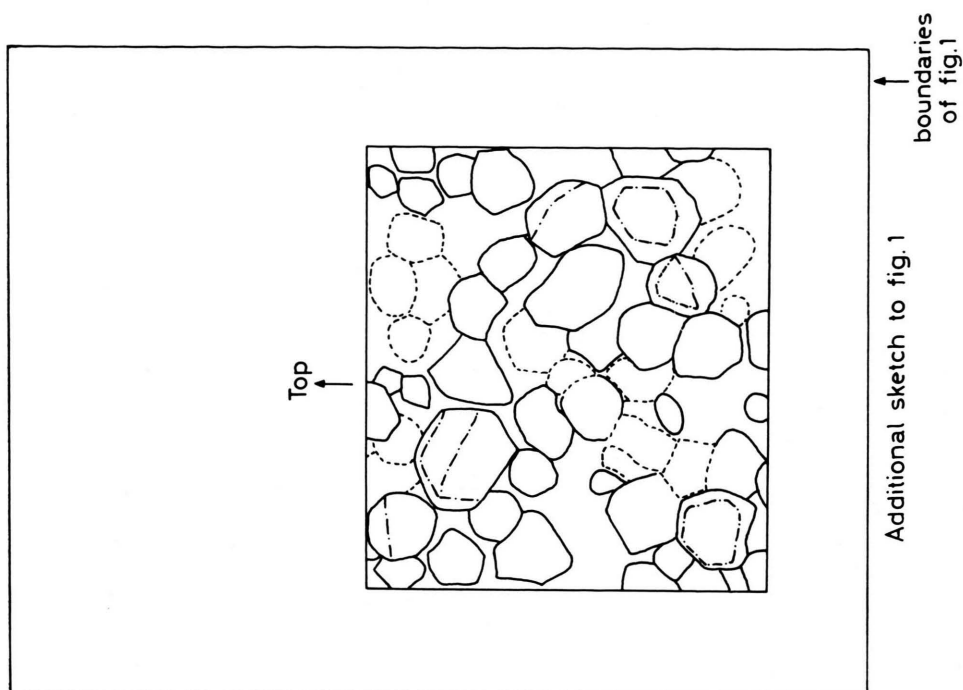


Fig. 1. Electron micrograph (direct Pt-C replica) of an unexposed photographic plate. In the additional sketch to Fig. 1, "visible" grains are indicated by full lines (—), clean cut edges between crystal planes by — · — · —, and "invisible" grains by - - - - -.

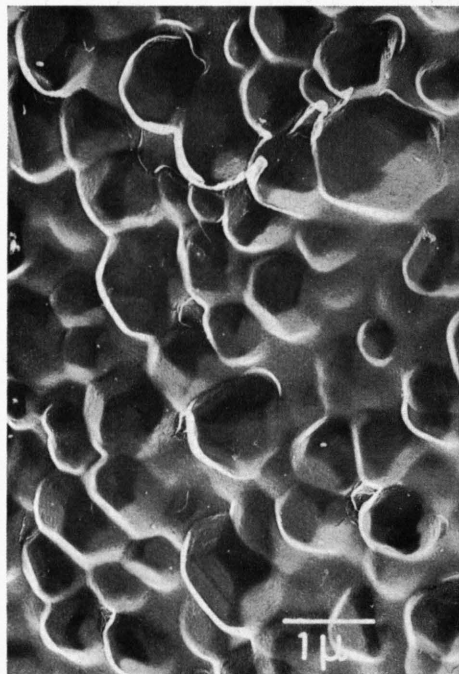


Fig. 1 a.

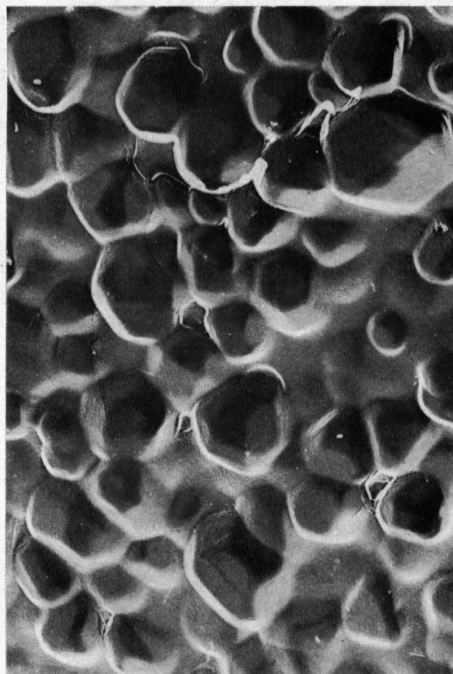


Fig. 1 b.

Fig. 1 a+1 b. Stereo electron micrographs (indirect Pt—C replicas) of an unexposed photographic plate. The hollows observed in these figures with a stereo viewer are due to the grains actually protruding from the gelatine matrix in the photoplate.

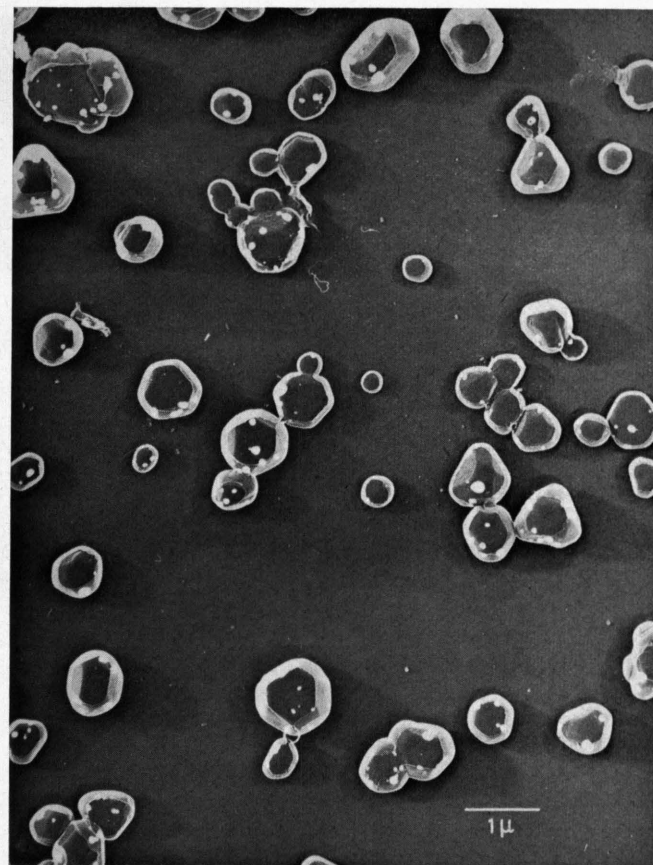


Fig. 3. Electron micrograph (direct Pt—C replica) of nude grains.

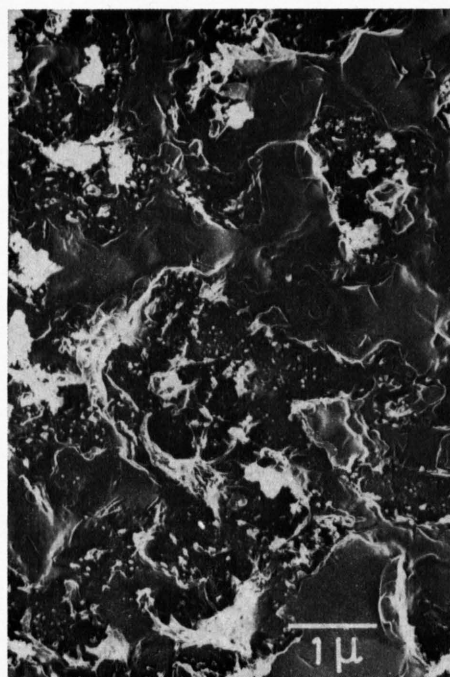


Fig. 5 a.

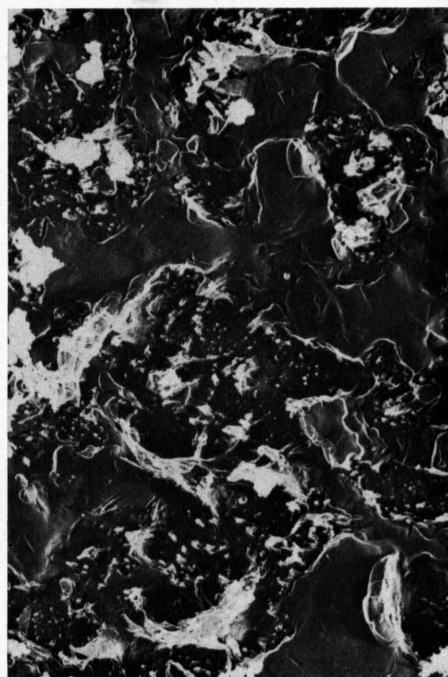


Fig. 5 b.



air

gelatine matrix

glassplate



Additional sketch to Fig. 5 b

Fig. 5 a and 5 b. Stereo photographs of part of Fig. 5, see p. 1036 d (indirect technovite Pt—C replicas). In the additional sketch to Fig. 5 b, the areas of the agglomerates, are indicated by full lines, the cross sections of the individual grains constituting these agglomerates by dotted lines.

Fig. 6. Enlarged photograph of a section (obtained by breaking the plate) through an actual photographic plate type Q2 (Ilford Ltd.). — Due to heavy atmospheric humidity while this photographic plate was studied, the average emulsion thickness as found from photographs like Fig. 6 is $2.5 \mu\text{m}$ and the thickness of the adhesion layer $0.6 \mu\text{m}$. The corresponding values for a dry emulsion are $1.9_5 \mu\text{m}$ and $0.5 \mu\text{m}$ respectively.

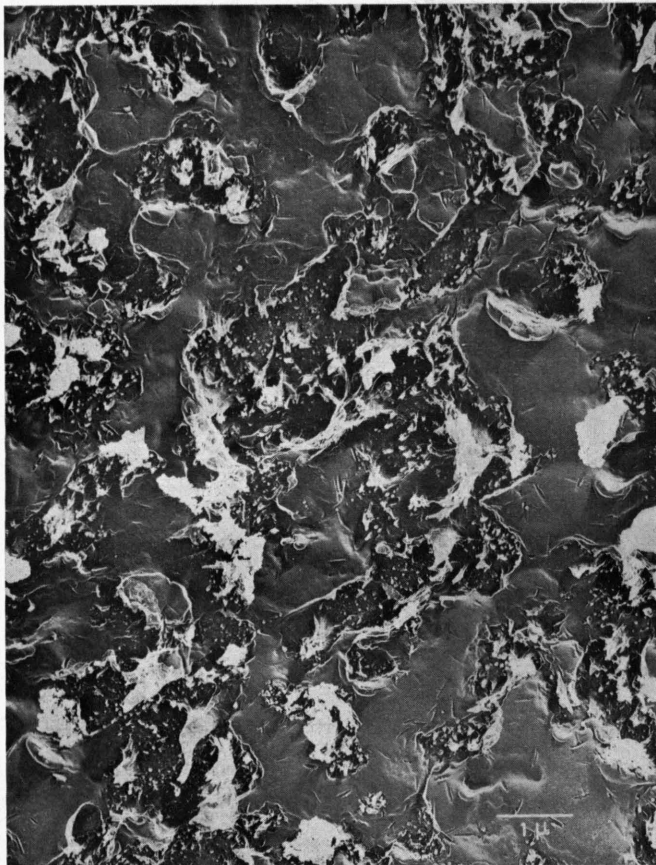


Fig. 5. Electron micrograph (indirect technovite Pt—C replica) of a photographic plate exposed to 17 keV carbon ions, developed and fixed.

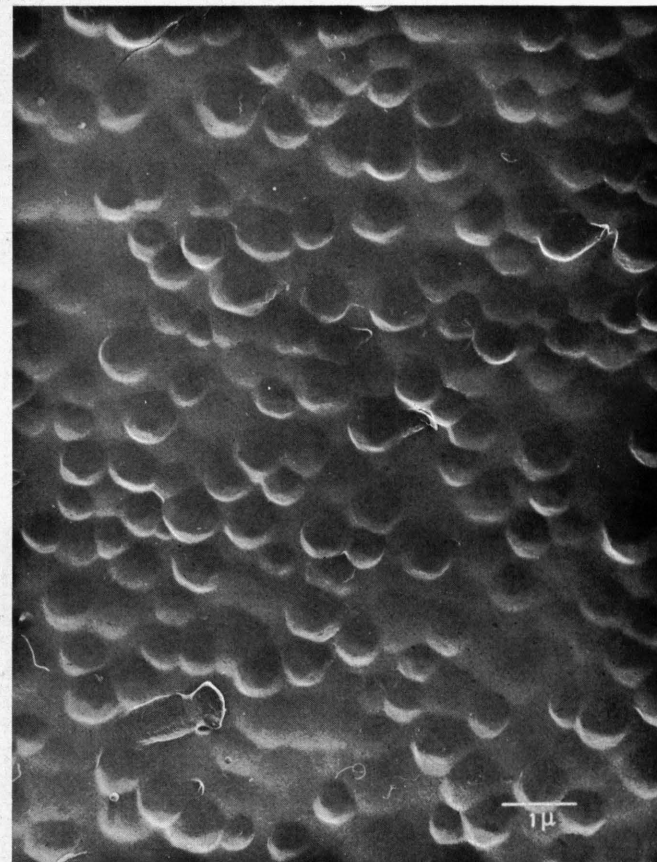


Fig. 8. Electron micrograph (indirect technovite Pt—C replica) of an unexposed photographic plate type Q1 (Ilford Ltd.).

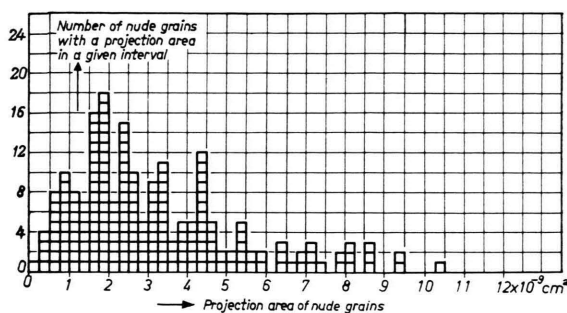


Fig. 4. Size-frequency distribution of nude grains.

we have followed in removing the gelatine, it must be concluded that the grains embedded in the gelatine matrix also are spherical. Because of the spherical shape of the grains, which protrude at least half-way out of the gelatine matrix, as can be seen from Figs. 1 and 1 a + 1 b and, D_0 being slightly greater than D_n , we may conclude that the grains are covered by a rather thin gelatine layer on the side facing the ions. From the difference between D_0 and D_n , the thickness of this layer was estimated to be about 250 \AA ¹². This value, however, can not be given with great accuracy owing to the uncertainty of this method.

Photographic Plates Exposed to Ions

Figs. 5 a and 5 b show stereo electron micrographs of a plate which was first exposed to 17 keV carbon ions, and then developed and fixed. From the examination of Figs. 5 a and 5 b with a stereo viewer one can see what appears like vast valleys surrounded by sometimes rather steep mountain ranges.

Since Figs. 5 a + 5 b are indirect replicas, the valleys seen here represent the protrusions where the Ag-agglomerates are left in the developed and fixed photographic plate.

The areas of the agglomerates, indicated by full lines in the additional sketch to Fig. 5 b, are found to be larger than the cross section ($4 \times 10^{-9} \text{ cm}^2$) of unexposed grains in the photographic plate. This is in good agreement with the photometric

values given by FRANZEN et al.³ who found for an average value ($R^2 = 0.35$) of the degree of subdivision of the agglomerate into grains an average grain-area of 10^{-8} cm^2 for exposed and developed Q2-plates. From careful stereo-examination of Figs. 5 a + 5 b, one can conclude that the agglomerates are mostly composed of several grains (indicated by dotted lines in the additional sketch), the cross-sections of which do not differ, much from the values found for unexposed grains. Small holes at the bottom of the valleys — as can be seen with a stereo viewer at least on the original photo — are due to threads of Ag that have pierced the gelatine layer above the grains during development. This could be ascribed to the loose structure or to the small thickness of that gelatine layer before or during development, or to a combination of both.

Emulsion Thickness

The emulsion thickness was measured with a Lichtschnittgerät¹⁴, Carl Zeiss, Jena at a step in the emulsion obtained by scratching away the gelatine matrix and subsequent vacuum deposition of a thin aluminium layer. We have measured the average emulsion thickness of a dried photographic plate as $1.95 \text{ }\mu\text{m}$.

The AgBr Areal Density

The average AgBr areal density η from five plates was found to be 0.33 mg/cm^2 , and that of dry gelatine 0.17 mg/cm^2 .

Distribution of the AgBr Grains in the Gelatine Matrix

An estimate of the grain distribution can be made using the areal density of AgBr, emulsion thickness, etc. Although these magnitudes have been determined from different spots on different plates (of the same batch), we may use them for this estimate because the values obtained within one plate and from other plates did not differ too much from each other.

¹² WAGNER¹³ has measured the thickness of this gelatine layer by examining microcuts of the emulsion under the electron microscope, and obtaining values between 200 and 400 \AA .

¹³ H. WAGNER, Frühjahrstagung der DPG, Regionalverband Bayern, Würzburg, April 1965.

¹⁴ In the „Lichtschnittgerät“ a parallel beam of light, after passing through a narrow slit, is allowed to strike the object at an angle of 45° . An unevenness, as in our case the step in the emulsion, throws a shadow. From the length of this shadow which is measured with a calibrated ocular incorporated in the „Lichtschnittgerät“, the height of the step can be calculated.

We had seen above that the fraction $a_0 G_0$ (a_0 = mean projection area, G_0 = mean number of grains/cm²) of the top layer of the emulsion covered with "visible" AgBr-grains is 0.70. As can be seen from Fig. 1, the AgBr-grains, being nearly spherical of average diameter D_0 and volume V_g , are arranged in one plane. A fraction $f \approx 0.75$ of these visible grains in the top layer, which can be called the upper top layer, lie about D_0 higher than the rest. The density of AgBr being $\rho = 6.4$ gr/cm³ we can calculate the areal density of the AgBr-grains in this upper top layer (average thickness D_0) from:

$$\eta = \rho V_g G_0 f = \rho G_0 f (4\pi/3) (D_0/2)^3 \\ = (2/3) \rho a_0 G_0 f D_0.$$

In this upper top layer of about $0.7 \mu\text{m}$ thickness we thus have about 0.16 mg/cm² of AgBr. The AgBr areal density in the dry emulsion about $2 \mu\text{m}$ in thickness has been determined as $\eta = 0.33$ mg/cm², from which we must conclude that the AgBr areal density in the remaining $1.3 \mu\text{m}$ thick layer is 0.17 mg/cm². This remaining layer consists of a nearly AgBr-free layer of gelatine (about $0.5 \mu\text{m}$ thick) adhering to the glass plate (see Fig. 6) and a gelatine layer of $0.8 \mu\text{m}$ thickness completely embedding the remaining AgBr-grains (0.17 mg/cm²).

A model of this AgBr distribution is shown in cross-section in Fig. 7.

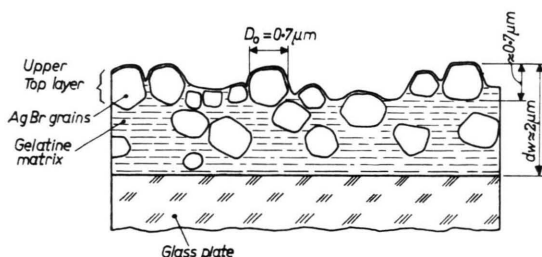


Fig. 7. Schematic drawing of the silver bromide distribution in the gelatine matrix of a photographic plate type Q2 (Ilford Ltd.).

Conclusion

The AgBr-grains of unexposed photographic plates (Type Q2, Ilford Ltd.) are mainly distributed in the upper layers of the gelatine matrix. The AgBr-

grains in the upper top layer protrude about halfway out of the gelatine matrix and are covered with a gelatine layer about 250 \AA thick on the surface. The gelatine layer adhering to the glass plate is found to be nearly free from AgBr.

These results show that the assumptions on the distribution of the grains in the gelatine matrix made by FRANZEN and SCHUY³ were correct. The first of our assumption made in ⁴ also is confirmed, viz. that the grains protrude at least halfway out of the gelatine matrix. Our second assumption was that the visible grains on the side facing the ions are covered by such a thin gelatine layer that all the ions, which impinge on the photoplate in the mass spectrometer are able to pass through this layer independently of their mass. This assumption seems, at first sight, not to be confirmed by our experiments: the thickness of the gelatine cover is about 250 \AA , which is greater than the penetration range, especially for the heavier ions in compact matter. MORBITZER¹⁵ e.g. reports a penetration range of 20 keV argon ions into calcium fluoride of 300 \AA , and LUTZ¹⁶ reports a 70 – 200 \AA penetration for 26 keV krypton ions into copper. As has been pointed out by WAGNER¹³, the penetration range of ions in gelatine can, however, be much greater due to the presence of cavities in such porous, macromolecular matter.

Measurements on gelatine-free ion-sensitive plates (l.c.^{17,18}) seem to confirm our ideas⁴ according to which the mass and energy-dependence of the sensitivity should not be affected by the gelatine cover, i.e. one should expect the same mass and energy-dependence of the sensitivity of gelatine-free plates as is found in plates in which the grains are embedded in gelatine. An energy-dependence of gelatine-free plates has been reported by WOOLSTON¹⁹. No measurements of mass-dependence of the sensitivity of this type of plate have been made, however, up to now. HONIG¹⁸ found an increase in sensitivity with increasing temperature, which he ascribes to an increase in the concentration of defects. This too, is in good agreement with our theory⁴.

From comparison of developed grains with unexposed grains we may conclude that photometric

¹⁵ L. MORBITZER and A. SCHARMANN, Z. Physik **181**, 67 [1964].

¹⁶ H. LUTZ and R. SIZMANN, Z. Naturforsch. **19a**, 1079 [1964].

¹⁷ M. H. HUNT, Anal. Chem. **38**, 620 [1966].

¹⁸ R. E. HONIG et al.: Gelatin-free Ion-sensitive Plates for Mass Spectrometers, Res. Rept. Sponsored in part by the Air Force Cambridge Research Laboratories, Aerospace Research, Contract No AF19 (628), 5106.

¹⁹ J. R. WOOLSTON and R. E. HONIG, 14th Mass Spectr. Conf. ASTM-E14, Dallas, May 1966.

determination of the area of developed grains will give slightly higher values than those obtained from electron micrographs of unexposed grains. This fact should be taken into account when the grain size is determined from photometric measurements.

We have dealt with Q2-plates (Ilford Ltd.) up to now. Some measurements have been carried out with Q1-plates (Ilford Ltd.) an electron micrograph of which is shown in Fig. 8.

The fraction of the area covered with visible grains was found to be 0.73, the average projection area being smaller than for Q2-plates.

Acknowledgement

The authors wish to thank Mr. ROEPERS for doing much of the numerical work and Mr. SCHELLING for the measurement of the emulsion thickness.

Ladungsträgerverluste in einem schwachionisierten stationären Gleichstromplasma im toroidalen Magnetfeld

F. KARGER

Max-Planck-Institut für Physik und Astrophysik, München

(Z. Naturforsch. 22 a, 1039—1057 [1967]; eingegangen am 14. März 1967)

For the particle losses of a weakly ionized plasma which result from the torus drift in a curved magnetic field, an expression is derived which is valid for certain parameters of the positive column of a gas discharge. To check this theory the "AMBIPOL" device was built. With this device it was possible to determine simultaneously the losses both in the toroidal and in the linear magnetic field by measuring the longitudinal electric field strength. As theory predicts, with growing magnetic field strength a weaker decrease of the longitudinal electric field was observed in the toroidal part of the discharge as compared to the linear part. The measured values of the relative electric field strength, however, exceed the theoretical limit, although the measurements of the electric field in the straight part and the measurements of the particle density and of the electron temperature in the curved part are consistent with theory. Moreover, contrary to the expectations, the onset of the KADOMTSEV instability occurs at lower critical magnetic fields in the toroidal part than in the straight part. Several possible explanations are discussed. In a later paper it will be attempted to make a choice among the three most probable ones.

A. Problemstellung und qualitativer Überblick

Der noch immer nicht völlig geklärte „Pump out“-Prozeß in Plasmamaschinen vom Typ des STELLARATORS gab den Anlaß, in einem Modell-Plasma den Einfluß der Krümmung des Entladungsrohres und der Magnetfeldlinien auf den Teilchenverlustmechanismus zu untersuchen. Als ein ohne allzu großen Aufwand herstellbares Laboratoriums-Plasma bot sich dabei die positive Säule einer stationären Niederdruck-Gasentladung mit nichtleitenden Wänden an.

In der Apparatur AMBIPOL (Abb. 1) wird die positive Säule mit überlagertem longitudinalen Magnetfeld in einen linearen (L) und einen toroidalen Anteil (T) aufgeteilt. (In den Abbildungen sind die Bezeichnungen L, T jeweils in einen Kreis gesetzt.) Die dadurch bedingte Gleichheit von Neutralgasdruck und Entladungsstrom in beiden Teilen erscheint als gute Basis für einen Vergleich zwischen

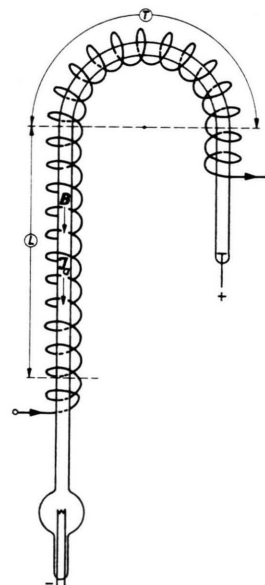


Abb. 1. Schema von AMBIPOL.